ENHANCING THE MICROSTRUCTURE AND MECHANICAL PROPERTIES OF CAST ALUMINUM MATRIX COMPOSITES THROUGH NANO-Al_2O_3 REINFORCEMENT VIA CMT AND PMC WELDING

Arzum Işıtan and Volkan Onar
Mechanical Engineering Department, Faculty of Technology, Pamukkale University, Kinikli, Denizli, Turkey

Süleyman Aytekin
Automotive Engineering Department, Faculty of Technology, Pamukkale University, Kinikli, Denizli, Turkey

https://doi.org/10.1007/s40962-023-01234-z

Abstract

In this investigation, two distinct composites were produced using the liquid metallurgy vortex-route method with an aluminum AA6013 matrix and 0.5% and 1% nano-Al_2O_3 reinforcement by weight. The effects of nano-Al_2O_3 ceramic particles added into the AA6013 alloy to increase the hardness and strength of the composite were investigated. Samples for welding were prepared from cast composite materials with dimensions of 250 × 110 × 60 mm. The obtained specimens were joined via butt welding at 110-A and 120-A current intensities, and at a constant speed of 400 mm/min by cold metal transfer (CMT) and pulse multi-control (PMC) welding methods. Using the use of micro- and macrostructural evaluations, hardness measurements, and tensile testing, the impacts of each welding parameter on the mechanical characteristics and weld structure of the cast composites were examined. The composite material with 0.5% nano-Al_2O_3 reinforcement that was joined at 120 A utilizing the CMT process achieved the highest tensile strength value at 96.6 MPa. At 110-A and 120-A welding current values, 0.5% reinforced composite demonstrated the maximum strength in both welding techniques.

Keywords: *nanocomposite, Al_2O_3, cold metal transfer (CMT) welding, pulse multi-control welding (PMC), aluminum matrix composite, mechanical properties*

Introduction

Modern materials technology enables the creation of components and systems that are significantly faster, lighter, more flexible, and more robust. With traditional materials, it is often difficult and even expensive to create parts that combine strength and lightness in a single material. This issue can be effectively addressed with composite materials, designed to overcome these challenges. Since reinforcement ratios and sizes, as well as the matrix material and reinforcement material types, can be altered, there is no limit to the variety of materials that can be produced by adding ceramic, polymer, and metal reinforcements to polymer, ceramic, and metal matrices. Within this broad material family, metal matrix composites in mechanical load-bearing applications and aluminum as a metal matrix composite (MMC) material come to the forefront. The 6xxx series aluminum alloys offer superior corrosion resistance compared to the traditionally widely used 2xxx and 7xxx alloys, and they are cost-effective. In addition to these properties, aluminum is an excellent matrix material for metal matrix composites due to its high formability and weldability. The most popular reinforcement materials used in MMC materials are Al_2O_3 and SiC. Aluminum matrix composite (AMC) reinforced with Al_2O_3 and SiC particles has advantages such as higher creep and wear resistance, as well as a higher strength-to-weight ratio compared to unreinforced aluminum alloy.[1,2]

Nanocomposites are created using reinforcement materials that are nanoscale in size. Studies show that nano-sized reinforcement reduces the grain size of the composite due to its high surface area/volume ratio, and thus, higher

Received: 01 September 2023 / Accepted: 01 December 2023
Published online: 08 January 2024

mechanical properties can be achieved by adding less reinforcement material. As an example, the mechanical properties of AMCs reinforced with 10% Al_2O_3 and 10% SiC by volume of microscale reinforcements were inferior to those of AMC reinforced with only 3% by vol. Al_2O_3 nanoparticles.[3,4]

Both liquid-state/fusion and solid-state welding methods can be used to join AMCs. During the fusion welding process, some problems that could result in low weldability, solidification cracking, or breakdown of ceramic particles could happen.[5] This is why solid-state welding techniques like friction stir welding (FSW) have been preferred and used for MMCs. By inserting various reinforcement materials, such as Al_2O_3, TiC, B_4C, and SiC onto various aluminum alloy matrices, such as AA 7005, 7075, and 6063, the weldability and mechanical properties of composites were investigated.[6–8] Nanoparticles are generally not put into the composite and are transported to the welding area, that is, to the weld seam, during the welding process. The process is called nano-doped aluminum FSW joints. Using the FSW method, Bahrami et al.[8] joined an AA7075/SiC nanocomposite. They obtained improved interfacial properties between the matrix material and the reinforcing material as well as a 76.1% improvement in tensile strength. In the study of Bodaghi and Dehghani,[9] it was found that the addition of SiC nanoparticles causes a considerable grain refinement of the welds in the AA5052/nano-SiC FSW application. In contrast with TiO_2 nanoparticles, Al_2O_3 nanoparticles demonstrated a fine recrystallized grain structure in the welding area in the work by Singh et al.[10] In comparison with the unreinforced welded material, the inclusion of nanoparticles boosted the material's microhardness, tensile strength, and wear resistance.

Solid-state welding exhibits superior metallurgical qualities. In contrast, it has drawbacks, including being unsuited for mass production, facing application challenges, having low efficiency, a lengthy welding process, and requiring a high initial investment cost.[10] Due to their advantages over other joining techniques, such as suitability for mass production, affordability, lack of part limitations during the welding process, and a quick welding process, liquid-state welding techniques such as tungsten inert gas (TIG), metal inert gas (MIG), and laser techniques have been widely used in the industrial sector. However, when welding of AMCs reinforced with ceramic particles using these methods, several unfavorable circumstances may arise due to the high heat input creation in the weld pool and the substantial thermal expansion of aluminum.[11,12]

In fusion welding processes, welding voltage, current, and pulse parameters impact on the heat input and droplet transfer. Controllable heat input is provided by the pulsed power supply, which has been in use for almost 60 years.[5,12] The pulse multi-control (PMC) welding method is a gas metal arc welding technique, which is based on the control of pulsed metal transfer and creates less heat input in the weld area compared to methods such as MIG and MIG-pulse methods.[13,14] Also, with a digitally controlled wire feeding system, the cold metal transfer (CMT) method, which controls material deposition and generates low heat input, can be used to weld aluminum without these drawbacks. CMT may also be utilized to weld various metals and thicker materials.[15] The PMC and CMT processes offer alternatives for materials that are difficult to weld due to needed high heat input, such as AMCs. In this area, addressing the part shape and size limitations that are considered disadvantages associated with FSW, researches are ongoing on liquid-state welding methods for joining AMCs. These methods can be used to prevent the development of undesirable microstructure and precipitates caused by high heat input.

For this purpose, in this study, nano-Al_2O_3 reinforced AMC material was produced by vortex-route method and welded via PMC and CMT welding methods using different welding currents. AA6013, which stands out in terms of toughness and strength compared to other 6XXX series alloys, was used as the matrix material. The microstructures, hardness, and mechanical properties of welded composite samples were investigated.

Material and Methods

In this study, the vortex-route casting method was used to create two distinct composites with an aluminum AA6013 matrix and 0.5% and 1% nano-Al_2O_3 reinforcement by weight.

AA6013 alloy exhibits good corrosion resistance and is well-suited for welding, heat treating, and forming, making it versatile for various applications. Table 1 provides information about the chemical composition of the alloy. The hardness value of the heat-treated and forged alloy is 149 HV, with tensile (Rm) and yield (Re) strengths of 379

Table 1. The Chemical Composition of the 6013 Alloy

Element	Si	Fe	Cu	Mn	Mg	Cr	Zn	Ti	Al
in wt. (%)	0.82	0.50	0.95	0.63	0.96	0.10	0.25	0.10	Bal.

and 359 MPa, respectively. The alloy finds common usage in rollerblade parts, hydraulic applications, valves, ABS brake systems, and machine parts.[16] In this study, the alloy was produced by casting to investigate the effects of nano-Al_2O_3 reinforcement on weldability.

Al_2O_3 is a ceramic material known for its high-temperature resistance. Its high modulus of elasticity and hardness make it a preferred reinforcing element in composite materials designed to operate at elevated temperatures where wear resistance is crucial.[17] In this study, 15-nm nano-Al_2O_3 powder with 99.5% purity was utilized as a reinforcement material.

To produce the AMCs, the AA6013 aluminum alloy was heated in the casting furnace up to 750 °C in stainless steel crucibles, each used separately for different mixing ratios, followed by slag removal. The nano-Al_2O_3 powder underwent heating in an electric furnace at 200 °C for an hour before being added to the molten AA6013 alloy in the casting furnace. Initially, the weight of the aluminum alloy was calculated and placed into the crucible. A 5.5-kg amount of AA6013 alloy was added to the furnace. The quantity of aluminum material to be melted was determined by adding the ingate volume to the model volume of the wooden model (dimensions of 250 × 110 × 60 mm) used in the sand mold, accounting for potential losses. Subsequently, the amount of reinforcement material was calculated and weighed as 27.5 g for a 0.5% reinforcement and 55 g for a 1% reinforcement ratio, utilizing a precision balance based on the weight ratio. A stainless steel stirrer was used for an hour in the casting furnace to ensure a homogenous mixture comprising the molten aluminum alloy and the reinforcement material (Figure 1).

Figure 1. The furnace used in casting process.

Green-sand molds were prepared for casting of the composite materials. Preliminary casting experiments were conducted on the design of the green-sand mold to observe and address issues such as solidification, formation of internal hollow structures, porosity, and mold filling challenges. Various model sizes, ingates, and risers were employed in these experiments (Figure 2). As a result of these studies, a mold design without riser was selected and used in the production of composites (Figure 3).

To prepare the welding samples, the ingates of the 250 × 110 × 60-mm cast composites were initially cut, and the rectangular prism-shaped ingots were mounted on a milling machine. All surfaces were cleaned by removing 5-mm chips for each surface. Composite materials reinforced with 0.5% and 1% nano-Al_2O_3 were sliced into dimensions of 3.5 × 100 × 50 mm, and samples were prepared for the welding process (Figure 4).

All surfaces of specimens were cleaned from cutting oil and chip dust, and then, the burrs from the cutting process were removed with felt. The samples prepared at a thickness of 3.5 mm and were butt-welded via CMT and PMC welding methods at Fronius International Company in Istanbul. A 1.2-mm diameter ER5183 (AlMg4.5Mn) welding wire was used in the welding process. The selection of welding wires took into account the chemical composition of AA6013. Argon gas was used as shielding gas at a flow rate of 12 l/min. The chemical composition of the wire used is provided in Table 2.

For each of the CMT and PMC welding methods, welded joints were conducted at two different current intensities, 110 and 120 A. Welding operations were carried out at a constant speed of 400 mm·min^{-1}. The heat input (H.I.) (J·mm^{-1}), generated during the welding process, was calculated according to Equation (1).[18] Welding parameters for all samples are given in Table 3, and welded specimens are shown in Figure 3.

$$H.I = (60 \cdot I \cdot V)/(\mathrm{FR}) \cdot \eta \left(J \cdot \mathrm{mm}^{-1}\right) \qquad \text{Eqn. 1}$$

where I: Current strength (Amps), V: Voltage (V), η: Arc efficiency, FR: Feed rate (mm·min^{-1}), and η (arc efficiency) is considered to be 0.8 for both CMT and PMC methods.[18]

The sections from the welded nanocomposites were cut and subsequently polished with diamond paste for investigations regarding the macrostructure and microstructure studies of the composite materials. Finally, Keller fluid was used for the etching process. Microstructures were examined with a microscope in the Pamukkale University Mechanical Engineering Metallography Laboratory. A Schottky field emission scanning electron microscope (FESEM) operating in high vacuum mode (HV) ($\leq 10^{-6}$ mbar) in ILTAM (Pamukkale University Advanced

Figure 2. Preliminary studies for green-sand mold design.

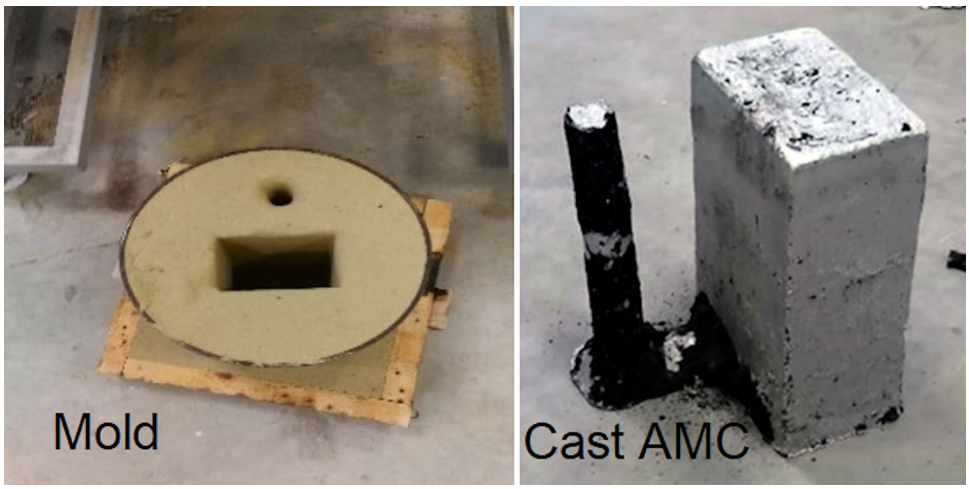

Figure 3. Cast composite material.

Figure 4. Cutting of cast composite material.

Material Research Center) was employed to characterize the welded and unwelded composites.

Phase analyses of the welded nano-Al_2O_3 reinforced composites were performed at Afyon Kocatepe University Technology Application and Research Center (TUAM) using a x-ray spectroscopy (XRD) Bruker D8 Advance diffractometer.

Tensile test specimens were formed by cutting flat bar specimens with dimensions of 3.5x20x140 mm from each welded composite in accordance with the DIN EN ISO 6892-1 standard[19]. Figure 5 illustrates the welded plates (a) and the tensile test specimens (b) cut from them. Tensile tests were conducted at a speed of 20 mm·min^{-1} on a 30-ton tensile test device.

Sample hardness values were determined at 12 different points, covering the middle of the weld zone, heat-affected zone (HAZ), and base material. The measurements were conducted under the conditions of a load application time of 5 seconds and a load of 200 grams (HV 0.2) (Figure 6).

Experimental Results

Tensile Test Results

The tensile test results of unwelded cast AA6013, AA6013+ 0.5% nano-Al_2O_3, and AA6013+ 1% nano-Al_2O_3 materials are presented in Table 4. The *R*m value of the AA6013 alloy in its as-cast form was determined as

Table 2. The Chemical Composition of ER5183 Welding Wire

Element	Al	Si	Mg	Mn	Fe	Cr	Cu	Zn	Ti
% in wt.	Bal.	<0.4	4.3–5.2	0.5–1.0	<0.4	<0.05	<0.1	<0.25	<0.15

Table 3. Welding Parameters

Material	Current (A)	Heat input ($kJ \cdot mm^{-1}$)		Speed ($mm \cdot min^{-1}$)	Wire
		CMT	PMC		
AA6013+ 0.5% nano-Al_2O_3	110	0.15	0.24	400	ER5183
AA6013+ 1% nano-Al_2O_3					
AA6013+ 0.5% nano-Al_2O_3	120	0.17	0.26		
AA6013+ 1% nano-Al_2O_3					

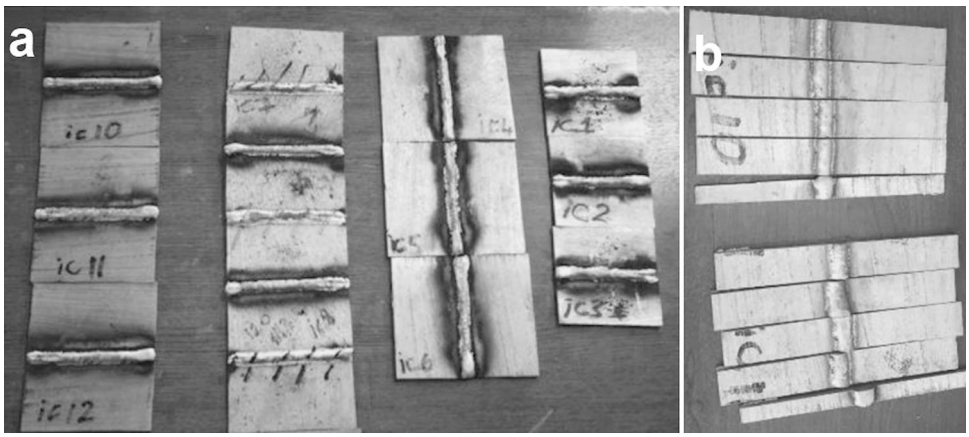

Figure 5. Welded plates and obtained tensile test specimens.

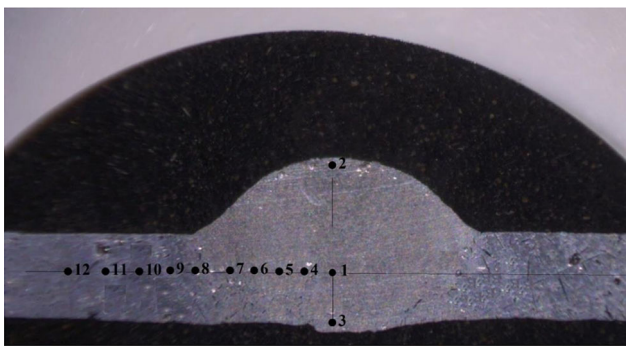

Figure 6. Hardness measurement.

Table 4. Tensile Test Results of Unwelded Specimens

Material	Ultimate stress, *R*m (MPa)	Yield stress, *R*e (MPa)	Elongation (%)
AA6013	83.73	67	0.95
AA6013+ 0.5% nano-Al_2O_3	95.48	76.58	1.17
AA6013+ 1% nano-Al_2O_3	89.52	72.4	0.82

83.73 MPa, and the Re value was 67 MPa. As mentioned in Section "Material and Methods," these values are lower than the values of the same alloy produced under forged and heat-treated conditions. It is a known fact that heat treatment and plastic deformation processes increase the strength of materials, and it is natural that they exhibit higher strength than cast materials.

The Rm and Re values obtained with nano-Al_2O_3 reinforcement showed an increase of 14% for 0.5%, and approximately 7% for 1% reinforcement ratios compared

Table 5. Tensile Test Results of Welded Specimens

Material		Method	Welding current (A)	Heat input (kJ·mm^{-1})	Ultimate stress, R_m (MPa)	Yield stress, R_e (MPa)	Elongation (%)
1	AA6013+ 0.5% nano-Al_2O_3	CMT	110	0.15	75.9	61.3	2.46
2	AA6013+ 0.5% nano-Al_2O_3		120	0.17	96.6	78	2.61
3	AA6013+ 1% nano-Al_2O_3		110	0.15	60.7	51.3	1.93
4	AA6013+ 1% nano-Al_2O_3		120	0.17	74.7	60	2.06
5	AA6013+ 0.5% nano-Al_2O_3	PMC	110	0.24	80.8	60.9	1.74
6	AA6013+ 0.5% nano-Al_2O_3		120	0.26	71.8	63.3	1.86
7	AA6013+ 1% nano-Al_2O_3		110	0.24	65.7	46.7	1.88
8	AA6013+ 1% nano-Al_2O_3		120	0.26	71.7	59.2	3.56

to the cast alloy without reinforcement. According to Shuvho et al.,[20] Al6063 MMCs reinforced with Al_2O_3, TiO_2, and SiC have higher tensile strength, hardness, and yield strength than pure Al6063, and all these characteristics improve as the ratio of reinforcing particles rises. In the study conducted by Chandrasekar and Nagaraju,[21] the porosity was reduced by 15.45% in a composite reinforced with coated Al_2O_3 particles compared to the as-cast scrap Al alloy. Also, the hardness, tensile strength, and impact strength were improved by 15.2, 23, and 31.25%, respectively.

Kumaresan ve Arul Kumar[17] indicated that the nanoparticles' reinforcement in AMC significantly improved the mechanical properties compared to the microparticles owing to their high surface energy. It was determined that when the reinforcement rate increased from 0.5 to 1%, the Rm value decreased by 7%, and the Re value decreased by 6%. Shayan et al.[22] determined that the mechanical properties of the AA2024-1vol%SiO_2np sample decreased compared to the AA2024-0.5 vol%SiO_2np sample due to agglomeration of nanoparticles and increased porosity. % elongation values are around 1% for all three samples. The tensile test results found in this study are consistent with the literature.

Tensile test results of welded composite materials are detailed in Table 5.

In the CMT method, as the welding current value increased from 110 to 120 A, the heat input value increased from 0.15 to 0.17 kJ·mm^{-1}. With the increase in heat input value, the tensile strength value (*R*m) of both composite materials increased. While the value obtained at 110-A current value in 0.5% nano-Al_2O_3 reinforced material was 75.9 MPa, the R_m value at 120 A increased by 27% to 96.6 MPa. Similarly, while the R_m value obtained at 110-A current value was 60.7 MPa in 1% nano-Al_2O_3 reinforced material, the *R*m value at 120 A was 74.7 MPa, indicating a 23% increase. The yield limit values (R_e) also increased similarly in parallel with increasing heat input values. While the value obtained at 110-A current in 0.5% nano-Al_2O_3 reinforced material was 61.3 MPa, the R_e value at 120 A increased by 27% to 78 MPa. The R_e value obtained at 110-A current was 51.3 MPa in 1% reinforced material, and the R_e value at 120 A was 60 MPa, showing a 16% increase. At a 0.15 kJ·mm^{-1} heat input condition, the 0.5% reinforced composite showed 25% more strength at the R_m value and 19% higher at the R_e value than the 1% reinforced composite. At a 0.17 kJ·mm^{-1} heat input condition, the 0.5% reinforced composite showed 29% more strength in R_m value and 30% more in R_e value compared to 1% reinforced composite.

In the PMC method, as the welding current value increased from 110 to 120 A, the heat input value increased from 0.24 to 0.26 kJ·mm^{-1}. Unlike the CMT method, the R_m value of 1% nano-Al_2O_3 reinforced composite materials increased, while the R_m value of 0.5% of nano-Al_2O_3 reinforced materials decreased. R_e values increased in both composites with increasing heat input in the PMC method. While the value obtained at 110-A current in 0.5% reinforced material was 80.8 MPa, the R_m value at 120 A decreased by 15% to 71.8 MPa. At 110-A current, the R_m value was 65.7 MPa in 1% reinforced material, and the *R*m at 120 A was 71.7 MPa, indicating a 9% increase. Concerning R_e, while the value obtained at 110-A current in 0.5% reinforced material was 60.9 MPa, the R_e at 120 A increased by 5% to 63.3 MPa. The R_e value obtained at 110-A current was 46.7 MPa in 1% reinforced material, the *R*e value at 120 A was 59.2 MPa, showing a 26% increase. At a 0.24 kJ·mm^{-1} heat input condition, the 0.5% reinforced composite showed 23% more strength at the R_m value and 30% higher at the R_e value than the 1% reinforced composite. At a 0.26 kJ·mm^{-1} heat input condition, the 0.5% nano-Al_2O_3 reinforced composite showed the same strength in the R_m value and 6% more in the R_e value compared to the 1% nano-Al_2O_3 reinforced composite.

Comparing the CMT and PMC methods, the highest R_m value of 96.6 MPa obtained in 0.5% nano-Al_2O_3 reinforced composite material, which was joined at 120 A using the

CMT method. The lowest R_m value in welding processes, 60.7 MPa, was obtained in 1% nano-Al_2O_3 reinforced composite material that was joined at 110 A by CMT method. In terms of R_e values, the highest R_e value was obtained as 78 MPa in 0.5% reinforced composite material via CMT method at 0.17 kJ·mm^{-1} heat input conditions. The lowest R_e value was obtained as 46.7 MPa in the PMC method in 1% reinforced composite under the condition of 0.24 kJ·mm^{-1} heat input.

Upon examining the tensile test results in general, it is observed that the 0.5% nano-Al_2O_3 reinforced composite showed higher strength in both welding methods and both current conditions. When the CMT method is used, the values obtained for 0.5% reinforced material reached a maximum level at 0.17 kJ·mm^{-1} heat input. It can be concluded that the increased heat input has a positive effect on the R_e and R_m strengths of composite materials in both welding methods except for the 0.5% nano-Al_2O_3 reinforced material's R_m value, which was welded via PMC method.

In the welding of AMCs, low heat input cannot provide the desired weld quality because sufficient penetration cannot be achieved in the weld. At high heat input values, on the other hand, distortions and residual stress formation may occur in the welded structure due to the high thermal expansion coefficient of aluminum. Additionally, as a result of the reactions between aluminum and ceramic particles, the uneven distribution of ceramic particles, the formation of oxide layers, undesirable microstructures, and precipitates may occur in the HAZ. Consequently, the microstructure, weld quality, and mechanical properties of welded AMCs are affected. It is stated in the literature that the strength of welded constructions of composite materials decreases with increasing heat input.[23,24] However, the dimensions of the reinforcement ceramic materials used in these studies were at the micron level. It is promising that when nano-sized reinforcement material is used, lower heat input value ranges and different welding methods can be used without decreasing mechanical properties.

The tensile test results of the unwelded and welded samples were remarkably close, especially at 120 A via CMT method, which yielded the highest mechanical properties for AA6013+ 0.5% nano-Al_2O_3. Moreover, the elongation at break value increased from 1.17 to 2.61%. This represents an extraordinary and novel development. As known, the strength of parts typically decreases, especially as a result of fusion welding processes, since the fusion zones typically exhibit coarse columnar grains due to the prevailing thermal conditions during the solidification of the weld metal. The tensile strength of welded samples can decrease by up to 50% compared to unwelded samples.[25,26] Incorporating nanoscale reinforcing material into the AMC can effectively address this issue.

Microstructural Characterization

Figure 7 presents the FESEM micrograph of the cast materials in order: Figure 7a: AA6013, Figure 7b: AA6013+0.5% nano-Al_2O_3, and Figure 7c: AA6013+1% nano-Al_2O_3. In the analysis, it was observed that Al_2O_3 nano-powders were dispersed without agglomeration in the composites. Superficial casting pores, which occurred in all composites, were not observed in the pure material. Structures consisting of Fe, Zn, Cr, Si, Ni, and Mg were formed as thin rod-like structures. A SEM-EDX analysis can be seen in the field analysis in Figure 8.

The welded samples underwent examination by optical microscope and FESEM to analyze the structure of the weld seam, the heat-affected zone (HAZ), and the base material, and the change of microstructure.

The microstructure image of CMT-welded 0.5% reinforced composite material at 110 A is depicted in Figure 9. In the welding process, a heat input of 0.15 kJ·mm^{-1} was generated. Although weld penetration occurred, the weld seam could not be obtained as desired. Large gas cavities were formed in the weld zone and in the HAZ. In the welding of AMCs, low heat input does not provide the desired weld quality as sufficient penetration cannot be achieved.[23]

The microstructure image of CMT-welded 0.5% reinforced composite material at 120-A welding current is shown in Figure 10. In the welding process, a heat input of 0.17 kJ·mm^{-1} was generated, and the weld penetration was well achieved. Compared to the sample welded at 110 A, gas gaps were observed less in the weld seam and HAZ.

For the 1% reinforced composite material welded with CMT at 110 A, the heat input is 0.15 kJ·mm^{-1}. In the weld seam and HAZ, large-scale gas cavities occurred, and the desired weld penetration could not be achieved (Figure 11a). When examining the 1% reinforced composite material welded via CMT at 120 A, which has a heat input of 0.17 kJ·mm^{-1} in the welding process, the weld penetration was not fully achieved (Figure 11c). There were small gas voids in the upper part of the weld zone, and cracks and voids occurred in the lower part (Figure 11b). Even though the 0.5% nano-reinforced welded materials were produced under the same casting conditions as the 1% nano-reinforced materials, fewer gaps and cracks appeared after welding process in the transition zone and welding area. This situation is also consistent with the mechanical test results. Consequently, it can be said that in the CMT welding method, the chemical composition has an effect on the weld structure and strength.

A well-formed welding structure was achieved, and small gas voids formed a porous structure in the 0.5% reinforced composite material welded at 110 A via PMC method. There was a heat input of 0.24 kJ·mm^{-1} in the welding

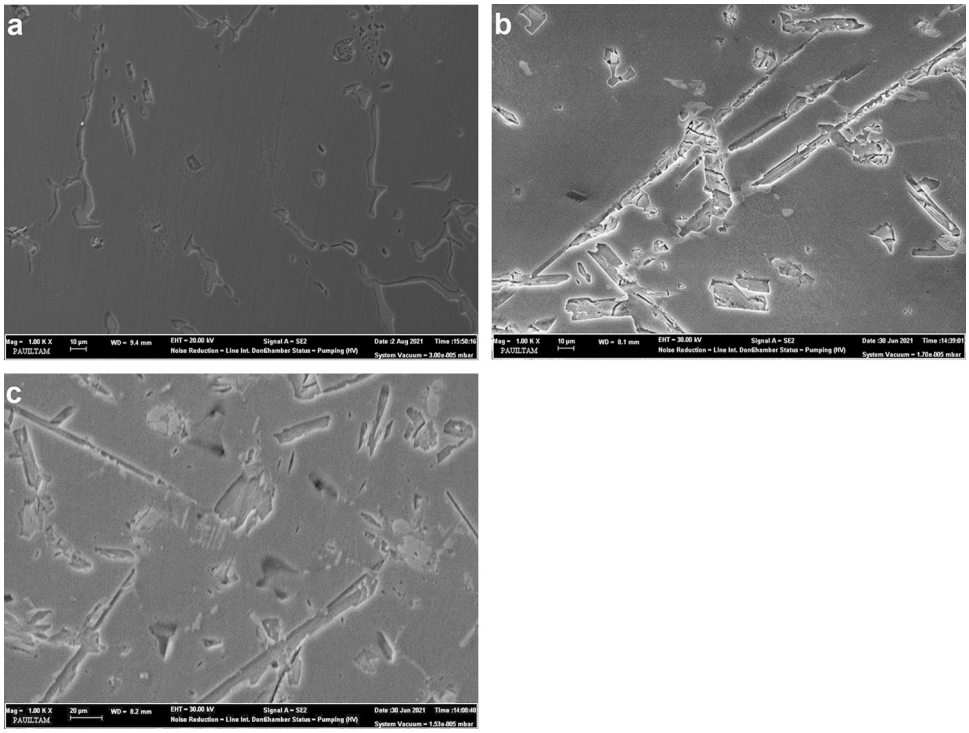

Figure 7. FESEM micrographs of cast materials (a) AA6013, (b) AA6013+0.5% nano-Al_2O_3, and (c) AA6013+1% nano-Al_2O_3.

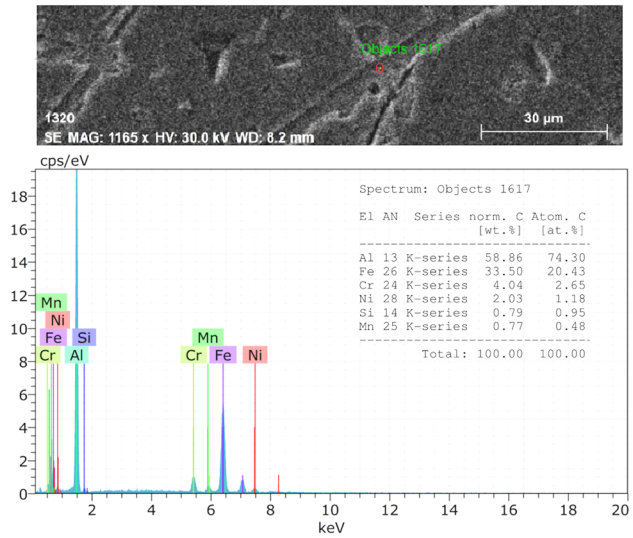

Figure 8. A point analysis of AA6013+1% nano-Al_2O_3 composite materials using SEM-EDX.

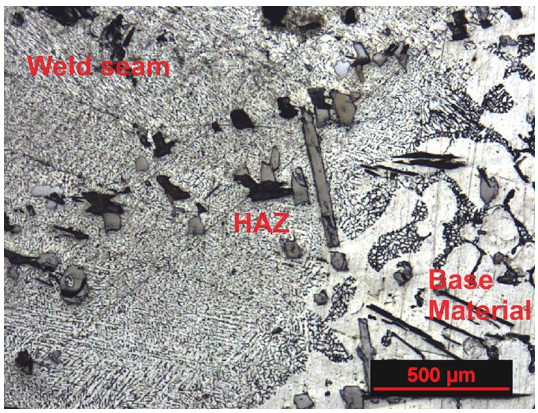

Figure 9. The microstructure image of the CMT-welded AA6013+0.5% nano-Al_2O_3 material at 110 A.

process. In contrast with other PMC-welded samples, there were fewer voids and less grain orientation obtained to the welding seam (Figure 12). A good weld penetration was observed in the microstructure examination of PMC-welded 0.5% reinforced composite material, which was welded at 120 A. There was a heat input of 0.26 kJ·mm^{-1} during the process. Besides gas voids in the weld area, cracks were formed in the HAZ (Figure 13a). For the 1% reinforced composite material joined at 110 A with PMC, there was a heat input of 0.24 kJ·mm^{-1} in the welding process. In addition to the formation of gas voids in the welding area, there was also a large void structure in the transition zone (Figure 13b). Weld penetration and the desired joining were not fully achieved for the 1% reinforced composite material welded at 120 A. There was a heat input of 0.26 kJ·mm^{-1} in the welding process. Large and small gas voids and cracks were intensively formed in the HAZ and welding area (Figure 13c).

Upon increasing the reinforcing ratio from 0.5 to 1%, the welded samples exhibited the formation of huge cavities. The findings of the tensile test show that these voids diminished the mechanical strength. Thus, it can be said that 0.5% reinforced material has less void formation and

more ideal microstructure characteristics. The study's findings demonstrate that various welding techniques can be applied to AMCs with nano-sized reinforcing material without lowering the mechanical properties or needing an extensive heat input.

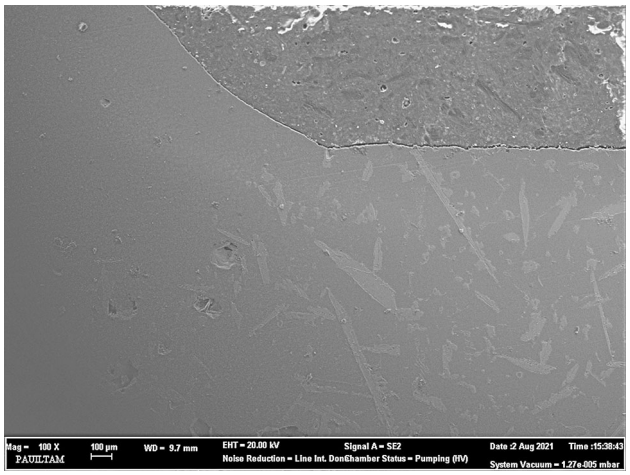

Figure 10. The FESEM image of the CMT-welded AA6013+0.5% nano-Al_2O_3 material at 120 A.

XRD Analyses of Welding Areas

In order to examine the phases formed in the welding area, the samples with the highest tensile strengths (CMT-welded AA6013+1% nano-Al_2O_3 material at 120 A and PMC-welded AA6013+0.5% nano-Al_2O_3 material at 110 A) were analyzed. In addition, the weld zone of the AA6013+1% nano-Al_2O_3 material at 110-A sample, welded via CMT, which has the lowest strength, was also analyzed.

Considering the lowest strength (CMT-welded AA6013+1% nano-Al_2O_3 at 110 A), it was determined that the $Al_{17}(Fe_{3.2}\ Mn_{0.8})Si_2$ phase was formed in the weld seam (Figure 14a). It is known that this phase precipitates at grain boundaries in aluminum alloys and reduces the mechanical properties of the alloy.[27] $Al_{0.985}\ Cu_{0.005}\ Mg_{0.01}$, $(Al_{26}\ Si)_{0.148}\ Al_{4.01}\ Mn\ Si_{0.74}$, and $Al_{11}\ Mn_{4.6}$ were also formed in the weld seam. Considering the chemical composition of both the main material and the welding wire, it is normal for these structures to form.[28]

Examining the sample with the second highest strength value (PMC-welded AA6013+0.5% nano-Al_2O_3 at 110 A), it was determined that $Al_{17}(Fe_{3.2}\ Mn_{0.8})Si_2$ phase was formed in the weld seam (Figure 14b). $(Al_{19}\ Zn)_{0.2}$, $(Al_{99}\ Si)_{0.04}$, and $(Al_{0.985}\ Cu_{0.005}\ Mg_{0.01})$ were also formed in the

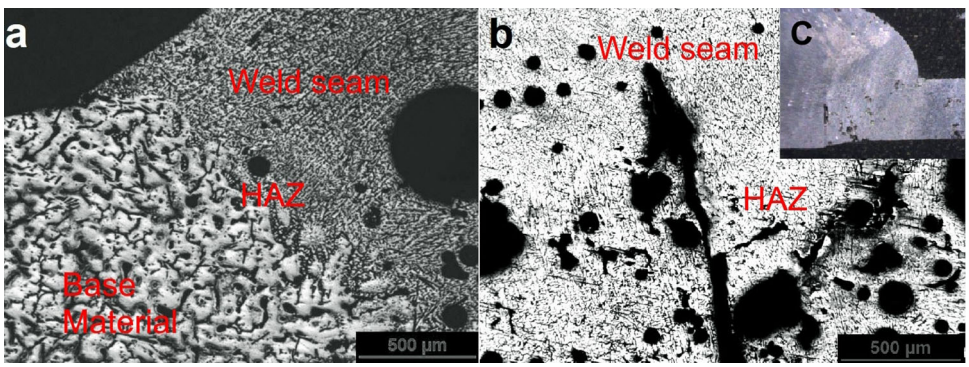

Figure 11. The microstructure image of the CMT-welded AA6013+1% nano-Al_2O_3 material at 110 A (a) and at 120 A (b).

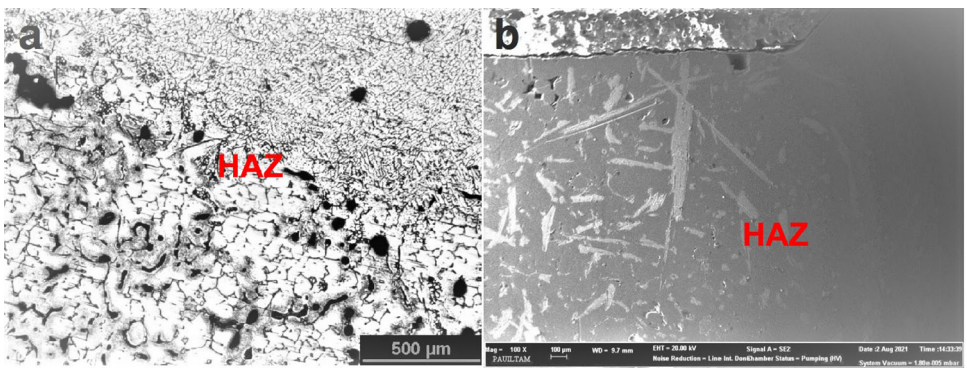

Figure 12. An optical (a) and a SEM (b) microstructure image of the PMC-welded AA6013+0.5% nano-Al_2O_3 material at 110 A.

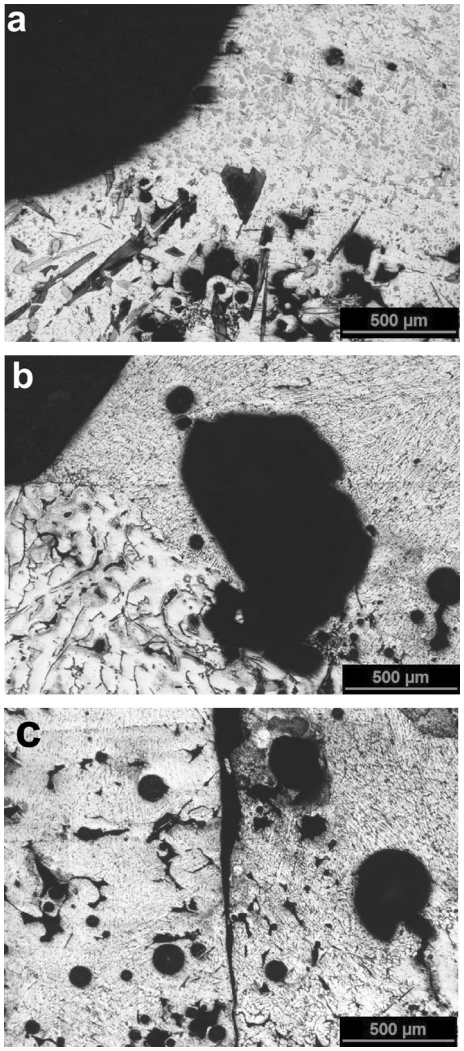

Figure 13. The microstructure images of the PMC-welded AA6013+0.5% nano-Al_2O_3 material at 120 A (a), AA6013+1% nano-Al_2O_3 material at 110 A (b), and AA6013+1% nano-Al_2O_3 material at 120 A (c).

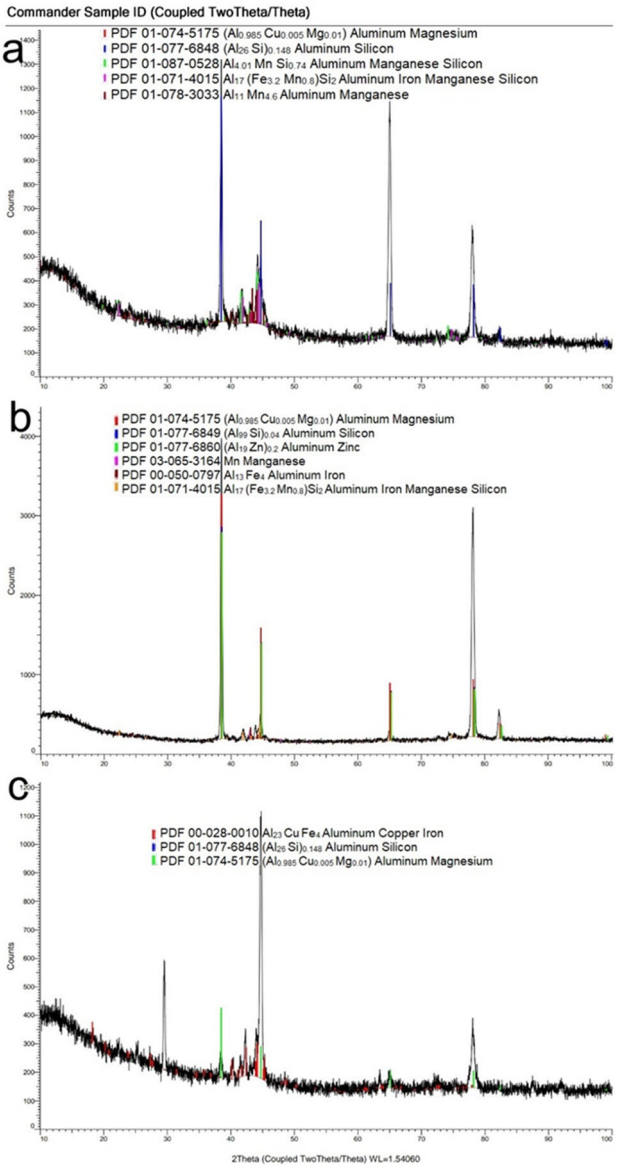

Figure 14. The XRD analyses of the CMT-welded AA6013+1% nano-Al_2O_3 at 110 A (a), PMC-welded AA6013+0.5% nano-Al_2O_3 at 110 A (b), and CMT-welded AA6013+0.5% nano-Al_2O_3 material at 120 A (c) .

weld seam. Considering the chemical composition of both the main material and the welding wire, it is normal for these structures to form except $(Al_{99}\ Si)_{0.04}$. In the study by Ebrahim et al.,[29] a surface mechanical alloying (SMA) with Si powder on Al at 600 °C was applied to achieve a surface composite. It has been determined that the formation of the Al-rich phase $(Al_{99}Si)_{0.04}$ cubic structure normally requires high temperatures and non-equilibrium conditions.

According to the phase investigations in the weld zone of the specimen with the highest strength value (CMT-welded AA6013+0.5% nano-Al_2O_3 at 120 A), $Al_{23}CuFe_4$, $(Al_{26}\ Si)_{0.148}$, and $Al_{0.985}\ Cu_{0.005}\ Mg_{0.01}$ formations were determined in the microstructure (Figure 14c). $Al_{17}(Fe_{3.2}\ Mn_{0.8})Si_2$ phase was not formed in this sample. The $Al_{23}CuFe_4$ intermetallic phase improves the mechanical properties of the alloys by creating precipitates as a result of heat treatments.[30]

XRD results reveal a 17% increase in strength compared to the closest welded sample as a result of the tensile test, depending on the phases formed as a result of the welding process. The formation of the $Al_{17}(Fe_{3.2}\ Mn_{0.8})$ phase embrittles the weld seam and reduces its strength. As shown in Figure 15a, it causes fracture at the weld seam. On the contrary, in the sample where the $Al_{23}CuFe_4$ intermetallic phase was formed, the fracture occurred in the transition zone, not in the weld seam (Figure 15b). On the contrary, the formation of $Al_{23}CuFe_4$ intermetallic phase reveals that the strength of the welded sample will increase further with the aging process. This indicates that the formation of the $Al_{23}CuFe_4$ intermetallic phase improves the mechanical properties of the alloy and shifts the fracture location from the weld seam to the transition zone.

Microhardness Results

The hardness values of the 0.5% reinforced composite, measured from the weld seam to the base metal, are presented in Figure 16. The composite that was welded by the CMT method at 110 A exhibited a lower hardness rating than the other samples. While the hardness value of the composite joined via CMT method at 110 A was lower than the other samples at 43.6 $HV_{0.2}$, the maximum hardness value in the weld seam was 58.8 $HV_{0.2}$. In the PMC method at a welding current of 110 A, a similar value was obtained. This value is almost the same as the weld seam hardness obtained at 120 A via CMT method (56.2 $HV_{0.2}$) and at 120 A via PMC method (58.4 $HV_{0.2}$). The maximum hardness value in the HAZ was obtained as 82.9 $HV_{0.2}$ for a PMC-welded sample at 110. However, when considering the overall hardness distribution of 0.5% reinforced composite CMT welded at 120 A, high hardness values are observed throughout the HAZ. It is known that there is a parallelism between the hardness of materials and their tensile strength. This can explain why the CMT-welded sample at 120-A welding current exhibits higher Rm strength compared to other samples.

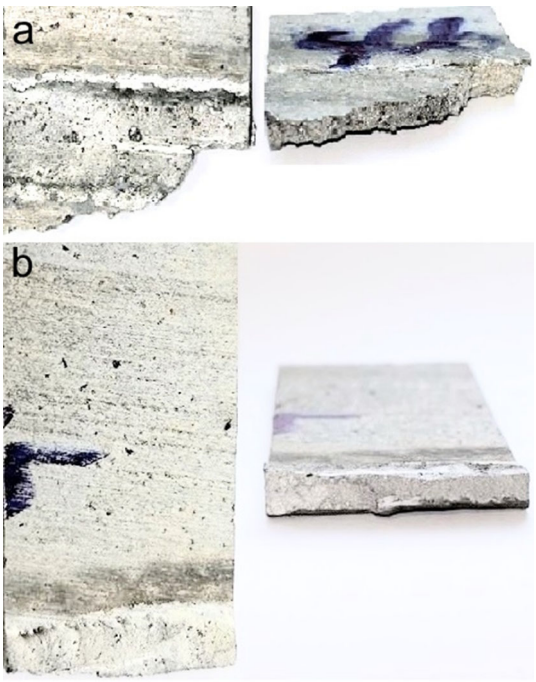

Figure 15. Images of the broken surfaces obtained as a result of the tensile test: (a) CMT-welded AA6013+1% nano-Al_2O_3 at 110 A and (b) CMT-welded AA6013+0.5% nano-Al_2O_3 material at 120 A.

Figure 17 illustrates the hardness values of 1% reinforced composite welded via CMT and PMC methods. At 110 A, hardness distribution does not show significant changes. However, the hardness values of the CMT-welded 1% reinforced composite at 120 A increased from the weld zone to the HAZ. While the hardness value of the composite in the weld seam via CMT method at 120 A was lower than the other samples, the maximum hardness value in the weld seam was obtained as 82 $HV_{0.2}$ via PMC method at 120 A. In the PMC method, the hardness values at the center of the weld seam were higher than in other zones. More heat input occurs in the PMC method at the same welding current value compared to the CMT method, and the hardness of the welding zone increases with the increase in the reinforcement ratio from 0.5% to 1%. Additionally, the hardness distribution obtained via CMT method is much more uniform than that obtained via PMC method. Therefore, based on these results, it can be concluded that the more homogeneous hardness distribution and the higher mechanical strength can be obtained depending on the reinforcement ratio.

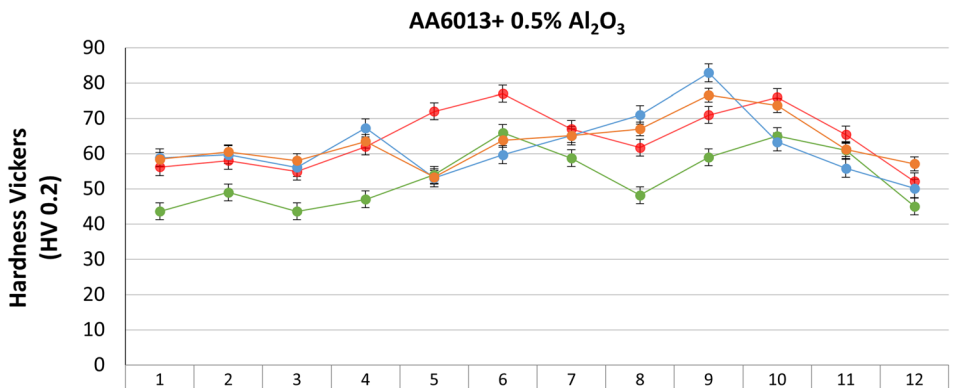

	1	2	3	4	5	6	7	8	9	10	11	12
CMT 110 A	43,6	49	43,6	47	54	65,9	58,7	48,2	59	65	61	45
CMT 120 A	56,2	58	54,9	62	72	77	67	61,7	71	76	65,4	52,1
PMC 110 A	58,8	59,7	56,1	67,3	53,1	59,7	65,1	71	82,9	63,3	55,8	50,1
PMC 120 A	58,4	60,5	58	63,5	53,3	63,8	65,1	67	76,6	73,7	61,2	57,1

Figure 16. Hardness distribution of 0.5% nano-Al_2O_3 reinforced composite.

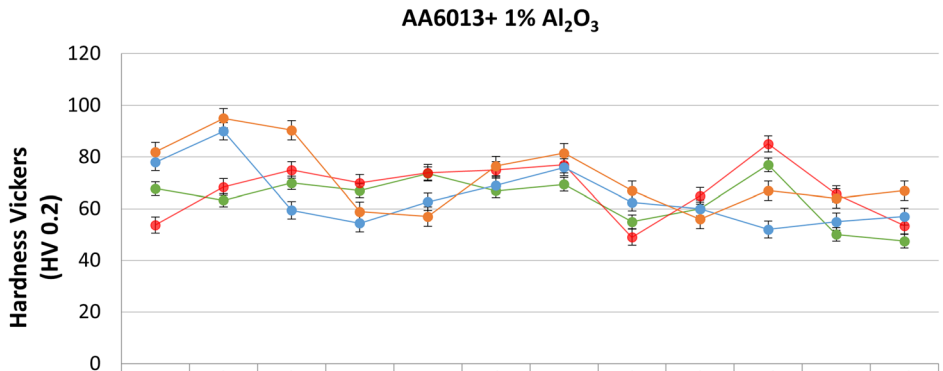

	1	2	3	4	5	6	7	8	9	10	11	12
CMT 110 A	67,8	63,3	70	67	73,6	66,9	69,4	55	60	77	50,1	47,5
CMT 1210 A	53,7	68,43	75	70	73,9	75	77	49	65	85,1	65,7	53,4
PMC 110 A	78	90	59,4	54,4	62,7	69	76	62,5	60	52	55	57
PMC 120 A	82	95	90,4	58,9	57	76,5	81,5	67	56	67	64	67

Figure 17. Hardness distribution of 1% nano-Al_2O_3 reinforced composite.

Conclusions

In this study, two distinct composites with aluminum AA6013 matrix and 0.5% and 1% nano-Al_2O_3 reinforcement by weight were produced using the vortex-route method. The cast specimens were welded via CMT and PMC techniques at constant speed of 400 mm/min and current intensities of 110 and 120 A. The effects of each welding parameter on mechanical characteristics and welding structure were examined using tensile and hardness tests. The microstructural characterization of these cast composites was investigated as well. The results of the studies carried out are summarized below:

(1) Al_2O_3 nano-powders were observed to be uniformly distributed throughout all composites without aggregating excessively.
(2) Cast samples welded via CMT and PMC welding methods, and the 0.5% nano-reinforced composites at 120-A showed less welding errors.
(3) The highest tensile and yield strengths were obtained as 96.6 MPa and 78 MPa, respectively, in the CMT-welded 0.5% nano-reinforced composite material at 120-A welding current.
(4) The obtained mechanical properties led to the conclusion that 0.5% Al_2O_3 reinforcement, as opposed to 1%, was ideal for welding of cast composites using both CMT and PMC methods.

Considering all these findings, the following recommendations for future research are provided:

(1) In this study, the mechanical properties of unaged cast samples were examined. Research can be conducted on how different aging conditions and different welding procedures affect the properties of cast composites.
(2) The mechanical properties of AA6013 used in this study were improved with nano-Al_2O_3. By creating various nano-reinforcement ratios below 1%, the best reinforcement ratios for casting and welding processes can be determined.

Acknowledgements

This study was supported by Pamukkale University Scientific Research Projects Unit (BAP) with project number 20FEBE040 as a Master Thesis titled "Analysis of the microstructure and hardness properties of aluminum matrix composite material reinforced with nano Al_2O_3 particles using different currents and forms of welding".[31]

Author Contributions AI took part in the casting process, microstructure investigations, and determination of mechanical properties. SA took part in the casting process, the processing and preparation of the samples, and the determination of the mechanical properties. VO took part in the welding process, preparation of samples, and determination of welding parameters.

Funding

Open access funding provided by the Scientific and Technological Research Council of Türkiye (TÜBITAK).

REFERENCES

1. P. Ajay Kumar, P. Rohatgi, D. Weiss, 50 years of foundry-produced metal matrix composites and future opportunities. Inter. Metalcast. **14**, 291–317 (2020). https://doi.org/10.1007/s40962-019-00375-4
2. M. Arumugam, M.S. Omkumar, M. Vinayagam, Mechanical and tribological characteristics of AA6082/ZrB2 composites. Mater. Test. (2021). https://doi.org/10.1515/mt-2020-0111
3. S.C. Tjong, Novel nanoparticle-reinforced metal matrix composites with enhanced mechanical properties. Adv. Eng. Mater. (2007). https://doi.org/10.1002/adem.200700106
4. W.H. Yu, S.L. Sing, C.K. Chua, C.N. Kuo, X.L. Tian, Particle-reinforced metal matrix nanocomposites fabricated by selective laser melting: a state of the art review. Prog. Mater. Sci. (2019). https://doi.org/10.1016/j.pmatsci.2019.04.006
5. P. Praveen, P. Yarlagadda, M.J. Kang, Advancements in pulse gas metal arc welding. J. Mater. Process. Technol. (2005). https://doi.org/10.1016/j.jmatprotec.2005.02.100
6. X.G. Chen, M. Da Silva, P. Gougeon, L. St-Georges, Microstructure and mechanical properties of friction stir welded AA6063–B4C metal matrix composites. Mater. Sci. Eng. A (2009). https://doi.org/10.1016/j.msea.2009.04.052
7. L. Ceschini, I. Boromei, G. Minak, A. Morri, F. Tarterini, Effect of friction stir welding on microstructure, tensile and fatigue properties of the AA7005/10 vol%Al_2O_3p composite. Compos. Sci. Technol. (2007). https://doi.org/10.1016/j.compscitech.2006.07.029
8. M. Bahrami, K. Dehghani, M.K.B. Givi, A novel approach to develop aluminum matrix nano-composite employing friction stir welding technique. Mater. Des. (2014). https://doi.org/10.1016/j.matdes.2013.07.006
9. M. Bodaghi, K. Dehghani, Friction stir welding of AA5052: the effects of SiC nano-particles addition. Int. J. Adv. Manuf. Technol. (2017). https://doi.org/10.1007/s00170-016-8959-8
10. T. Singh, S.K. Tiwari, D.K. Shukla, Mechanical and microstructural characterization of friction stir welded AA6061-T6 joints reinforced with nano-sized particles. Mater Charact (2020). https://doi.org/10.1016/j.matchar.2019.110047
11. P. Bassani, E. Capello, D. Colombo, B. Previtali, M. Vedani, Effect of process parameters on bead properties of A359/SiC MMCs welded by laser. Compos. Part A Appl. Sci. Manuf. (2007). https://doi.org/10.1016/j.compositesa.2006.04.014
12. K. Mutombo, M. Du Toit, Corrosion fatigue behaviour of aluminium alloy 6061–T651 welded using fully automatic gas metal arc welding and ER5183 filler alloy. Int. J. Fatigue (2011). https://doi.org/10.1016/j.ijfatigue.2011.06.012
13. Gomes, B.F., Morais, P.J., Ferreira, V., Pinto, M., Almeida, L.H. Wire-arc Additive Manufacturing of Al-Mg Alloy Using CMT and PMC Technologies. in: 8th EASN-CEAS International Workshop on Manufacturing for Growth & Innovation (2018). https://doi.org/10.1051/matecconf/201823300031
14. Fronius. Pulse Multi Control: Kontrollü Ve Hızlı Kaynaklama Için Yeni Impuls. https://www.fronius.com/tr-tr/turkey/kaynak-teknolojisi/kaynak-duenyas/fronius-welding-processes/pmc
15. C.G. Pickin, K. Young, Evaluation of cold metal transfer (CMT) process for welding aluminium alloy. Sci. Technol. Weld. (2006). https://doi.org/10.1179/174329306X120886
16. Matweb, Aluminum 6013-T651 Characteristics and Uses. https://www.matweb.com/search/datasheet_print.aspx?matguid=30c783afc390492f9dfdcc36315f0fc0
17. G. Kumaresan, Arul kumar, B., Investigations on mechanical properties of micro- and nano-particulates (Al_2O_3/B_4C) reinforced in Al 7075 matrix composite. Inter. Metalcast. (2022). https://doi.org/10.1007/s40962-021-00741-1
18. B.Y. Dharmik, N.K. Lautre, CMT and GTA welding on microstructural characteristics and magnetic performance of thin CRNO electrical steel sheets. Mater. Chem. Phys. (2023). https://doi.org/10.1016/j.matchemphys.2022.127128
19. DIN EN ISO 6892-1, 2020 Edition, June 2020- Metallic materials- Tensile testing- Part 1: Method of test at room temperature (ISO 6892-1:2019)
20. M.B. Shuvho, M.A. Chowdhury, M. Kchaou, B.K. Roy, A. Rahman, M.A. Islam, Surface characterization and mechanical behavior of aluminum based metal matrix composite reinforced with nano Al_2O_3, SiC, TiO_2 particles. Chem. Data Collect. (2020). https://doi.org/10.1016/j.cdc.2020.100442
21. P. Chandrasekar, D. Nagaraju, The effect of electroless Ni–P-coated Al_2O_3 on mechanical and tribological properties of scrap Al Alloy MMCs. Inter. Metalcast. (2022). https://doi.org/10.1007/s40962-022-00779-9
22. M. Shayan, B. Eghbali, B. Niroumand, Synthesis and characterization of Aa2024-SiO^2 nanocomposites through the vortex method. Inter. Metalcast. (2021). https://doi.org/10.1007/s40962-021-00574-y
23. A. Urena, M.D. Escalera, L. Gil, Influence of interface reactions on fracture mechanisms in TIG arc-welded aluminium matrix composites. Compos. Sci. Technol.

(2000). https://doi.org/10.1016/S0266-3538(99)00168-2
24. M.B.D. Ellis, Joining of aluminium based metal matrix composites. Int. Mater. Rev. (1996). https://doi.org/10.1179/imr.1996.41.2.41
25. A.K. Lakshminarayanan, V. Balasubramanian, K. Elangovan, Effect of welding processes on tensile properties of AA6061 aluminium alloy joints. Int. J. Adv. Manuf. Technol. (2009). https://doi.org/10.1007/s00170-007-1325-0
26. V. Balasubramanian, V. Ravisankar, G. Madhusudhan Reddy, Effect of pulsed current welding on mechanical properties of high strength aluminum alloy. Int. J. Adv. Manuf. Technol. (2008). https://doi.org/10.1007/s00170-006-0848-0
27. A.R. Eivani, H. Ahmed, J. Zhou, J. Duszczyk, Modeling the TDFD dissolution of Al–Fe–Mn–Si particles in an Al–4.5 Zn–1Mg alloy. Philos. Mag. (2010). https://doi.org/10.1080/14786431003662580
28. A. Uluköy, Pulsed metall inert gas (MIG) welding and its effects on the microstructure and element distribution of an aluminum matrix reinforced with SiC composite material. Materialwiss Werks (2017). https://doi.org/10.1002/mawe.201700568
29. M.R. Ebrahim, A.M. Labeeb, I. Battisha, Electrical properties of Al-Si surface composites through surface mechanical alloying on severe plastic deformed Al substrates. J. Alloys Compd. (2023). https://doi.org/10.1016/j.jallcom.2023.170925
30. A.E.A. Chemin, C.M. Afonso, F.A. Pascoal, C.D.S. Maciel, C.O.F.T. Ruchert, W.W. Bose Filho, Characterization of phases, tensile properties, and fracture toughness in aircraft-grade aluminum alloys. Mater. Des. Process. Commun. (2019). https://doi.org/10.1002/mdp2.79
31. Aytekin, S. Analysis of the microstructure and hardness properties of aluminum matrix composite material reinforced with nano Al_2O_3 particles using different currents and forms of welding, Master's thesis, Pamukkale Üniversitesi Fen Bilimleri Enstitüsü (2021).